Optics Communications xx (xxxx) xxxx–xxxx

Contents lists available at ScienceDirect

Optics Communications

journal homepage: www.elsevier.com/locate/optcom

Capacity of arbitrary-order orbital angular momentum multiplexing system

Yaqin Zhao*, Xin Zhong, Guanghui Ren, Shengyang He, Zhilu Wu

School of Electronics and Information Engineering, Harbin Institute of Technology, P.O. Box 342, No. 92, West Da-Zhi Street, Harbin 150001, Heilongjiang, China

ARTICLE INFO

2010 MSC:
94A14
94A15
94A40

Keywords:
Orbital angular momentum
Multiplexing
Capacity
Spectral efficiency
Cross correlation

ABSTRACT

Arbitrary-order orbital angular momentum multiplexing (AOAMM) systems utilize OAM modes with both integer and fractional topological charges which are non-orthogonal. In this paper, the transmission matrix and the capacity per unit bandwidth, i.e., the spectral efficiency (SE) of an AOAMM system is derived based on the spatial cross correlations of the OAM submodes under different aperture conditions. The results show that in limited apertures, the SEs of AOAMM systems increase dramatically as the interval of two adjacent OAM submodes decreases by losing orthogonality. AOAMM systems are effective choices for satisfying the explosive growth of the communication requirements. This paper provides insight into the selection of spatially multiplexing approaches and the design of interference mitigation techniques for AOAMM systems with increased SEs.

1. Introduction

Since the beginning of the 1990s, light beams with orbital angular momentums (OAM) have received much attention [1]. Extensive researches have been conducted in the applications of OAM beams, such as manipulating particles, quantum information, communications, etc. [2–6]. Most research focuses on the beams with integer OAMs, because of the orthogonality and the infinite set of orthogonal bases in theory [7–9]. However, as the OAM increases, the radius of the beam turns larger. Sequentially, high-order OAM beams are not suitable for integrated silicon photonics OAM devices [10]. Besides, the capacity of the orthogonal OAM multiplexing system is limited by finite transmitting/receiving apertures and is outperformed by spatial mode multiplexing (SMM) systems [11]. Abderrahmen Trichili et al. showed that in OAM-based multiplexing systems, the detection apertures affect the system performance less than the transmitting and receiving apertures [12]. Then the applications of orthogonal OAM modes are limited.

As the requirements of communications growing explosively, some researchers have proposed non-orthogonal multiplexing access (NOMA) schemes, which compose one of the key branches of the 5th generation (5G) communications, in order to utilize the wireless spectrum more efficiently [13–15]. Safa Isam et al. proposed spectrally efficient frequency division multiplex (SEFDM) [16]. It is also one of the NOMA schemes. These researches have shown us the viability of non-orthogonal signals and inspire us to put more focus on non-orthogonal OAM modes.

OAM beams with fractional topological charges offer more potential dense information carriers to overcome the limitation of the apertures. They have already been studied for optical communication systems [17–19]. To the best of our knowledge, the systems using beams with OAM channel interval of less than 0.5 have not been investigated. To date, the smallest OAM channel interval used in fractional OAM communication systems is 0.6 [20]. Highly pure OAM modes with continuously varying topological charges make the beams with very small OAM channel intervals available [21–23]. Arbitrary-order OAM multiplexing (AOAMM) systems utilize non-orthogonal OAM modes with both integer and fractional topological charges simultaneously. On the contrary, the systems that only utilize integer OAM beams are orthogonal. To detect non-orthogonal signals, several approaches have already been developed. These approaches include maximal likelihood (ML) detector, truncated singular value decomposition (TSVD) and sphere decoder (SD), etc. [16,24–26]. These techniques need to be modified to satisfy the requirements of AOAMM systems in future works. Besides, spatial cross correlation is another effective way to process non-orthogonal signals. Cross correlations depict the level of interference among different OAM beams and present the mode processing gain in the systems using optical correlators and the work of Jesus et al. provided insight into mutual interference among the submodes of OAM multiplexing systems [27].

The work in this paper focuses on analyzing the capacity limits of the AOAMM system using OAM submodes with intervals of less than

* Corresponding author.
E-mail address: yaqinzhao@hit.edu.cn (Y. Zhao).

http://dx.doi.org/10.1016/j.optcom.2016.10.069
Received 3 August 2016; Received in revised form 17 October 2016; Accepted 25 October 2016
Available online xxxx
0030-4018/

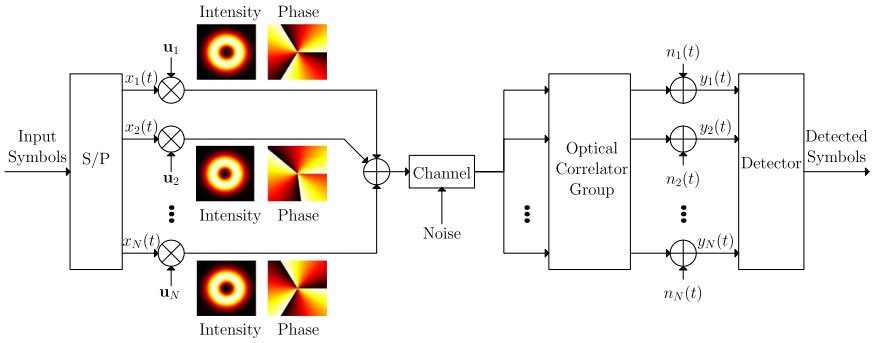

Fig. 1. System model of the AOAMM system. The topological charges of the exampled OAM submodes range from −3 to 3 with the interval of 0.4 and N=16. The component S/P is the serial-to-parallel converter.

0.5 and is organized as follows. The system model is proposed in detail in Section 2, including the signal structure, the channel model, the detections of the received signal and some other discussions. In Section 3, the spectral efficiencies of the AOAMM systems with different detection techniques are discussed. The simulation results are presented in Sections 4 and 5 draws the conclusion.

2. Model of AOAMM system

The structure of the AOAMM system is similar to the orthogonal OAM multiplexing system. The differences are the OAM submodes and the detection techniques. The AOAMM system uses both fractional and integer OAM submodes and requires techniques to process non-orthogonal multiplexed signals. According to the structures in [9,28], the model of the AOAMM system can be presented as Fig. 1, together with the field distributions of the arbitray-order OAM submodes at the initial plane.

The essential feature of the AOAMM system is the usage of the OAM submodes with topological charge intervals of less than 1 as is shown in Fig. 1. The input symbols are split into N paths, i.e., $\{x_1(t), x_2(t), \ldots, x_N(t)\}$. Each path of the symbols is carried by a specific OAM submode described by the field distribution $\mathbf{u}_n$, $n \in 1, 2, \ldots, N$. Then all the modulated signals are summed together to be transmitted. For OAM-based multiplexing systems, the singular values of their transmission matrices show that the OAM submodes satisfying the space-bandwidth product limits can transmit almost all the energy through the channels [11]. The channel is a distance of free space. The noise is the additive white Gaussian noise. The receiver splits the received signal into N paths and processes the signal with a group of optical correlators. The outputs of the optical correlators are $\{y_1(t), y_2(t), \ldots, y_N(t)\}$, defined as the received signal vector $\mathbf{Y}(t)$.

Laguerre-Gaussian (LG) beams with radial index of 0 are the most typical OAM beams. An LG OAM beam $\mathbf{u}_n$ with topological charge l_n is given by

$$\mathbf{u}_n = U_n \left(\frac{r}{\omega_0}\right)^{|l_n|} \exp\left(-\frac{r^2}{\omega_0^2}\right) \exp(-il_n\theta) \tag{1}$$

where U_n is the amplitude constant, ω_0 is the Gaussian beam waist at z=0, r is the cylindrical radius, and θ is the azimuthal angle. Let Δl be the topological charge interval between two adjacent LG beams.

2.1. Signal structure

The modulated signals are

$$\mathbf{u}_{n,mod} = x_n U_n \left(\frac{r}{\omega_0}\right)^{n} \exp\left(-\frac{r^2}{\omega_0^2}\right) \exp(-il_n\theta),\ n \in 1, 2, \ldots, N \tag{2}$$

The signal at the transmitting aperture is the sum of the modulated OAM submodes, expressed as

$$\mathbf{u}_o = \sum_{n=1}^{N} \mathbf{u}_{n,mod}. \tag{3}$$

Then the summed light beam is transmitted through an optical transmitting aperture. It is usually a lens system.

2.2. Free space channel

In practical free-space optical links, the propagation satisfies the Huygens-Fresnel principle [29]. Considering different propagation distances, the free-space propagation can be modeled as the Fresnel diffraction and the Fraunhofer diffraction, respectively. The near-field propagation is modeled as the Fresnel diffraction, expressed as

$$\begin{aligned} U(x, y, z) = {} & \frac{\exp(ikz)}{i\lambda z} \exp\left[\frac{ik}{2z}(x^2 + y^2)\right] \cdot \\ & \iint \left\{ U(\xi, \eta, 0) \exp\left[\frac{ik}{2z}(\xi^2 + \eta^2)\right] \right\} \cdot \\ & \exp\left[-i2\pi\left(\frac{x\xi}{\lambda z} + \frac{y\eta}{\lambda z}\right)\right] d\xi d\eta. \end{aligned} \tag{4}$$

The far-field propagation is modeled as the Fraunhofer diffraction, expressed as

$$\begin{aligned} U(x, y, z) = {} & \frac{\exp(ikz)}{i\lambda z} \exp\left[\frac{ik}{2z}(x^2 + y^2)\right] \cdot \\ & \iint U(\xi, \eta, 0) \cdot \\ & \exp\left[-i2\pi\left(\frac{x\xi}{\lambda z} + \frac{y\eta}{\lambda z}\right)\right] d\xi d\eta \end{aligned} \tag{5}$$

Pierre Pellat-Finet has already proved that the Fractional-order Fourier transforms are adapted to the mathematical expression of Fresnel diffraction, just as the standard Fourier transform is adapted to Fraunhofer diffraction [30].

After derivations based on the analysis in [30], the beam transmitted through a distance z of free space can be recovered based on the relations

$$\begin{cases} \widetilde{U}(\xi, \eta) = \mathcal{F}^{-p}\{\Theta_n U(x, y, z)\}, & \text{for near field,} \\ \widetilde{U}(\xi, \eta) = \mathcal{F}^{-1}\{\Theta_f U(x, y, z)\}, & \text{for far field.} \end{cases} \tag{6}$$

where Θ_n and Θ_f are defined as

$$\begin{cases} \Theta_n = \dfrac{i\lambda z}{\exp(ikz)\cos\phi} \exp\left[\dfrac{-ik}{2z}(x^2 + y^2)\tan\phi\right], \\ \Theta_f = \dfrac{i\lambda z}{\exp(ikz)} \exp\left[\dfrac{-ik}{2z}(x^2 + y^2)\right]. \end{cases}$$

In Eq. (6), $\phi = p\pi/2$, $\mathcal{F}^{-p}\{\cdot\}$ denotes the inverse Fractional-order Fourier transform of order p and $\mathcal{F}^{-1}\{\cdot\}$ denotes the inverse Fourier transform. They both can be implemented by lenses [18].

We simulate the propagation of a fractional OAM beam and a integer OAM beam, as well as the recovery process. The results are shown in Fig. 2. For more details about the fractional Fourier transformation of fractional OAM beams, readers can refer to the